

Field-tuning of the electron and hole populations in the ruthenate $\text{Bi}_3\text{Ru}_3\text{O}_{11}$

Wei-Li Lee,¹ M. K. Haas,² G. Lawes,³ A. P. Ramirez,³ R. J. Cava,^{2,4} and N. P. Ong^{1,4}

¹Department of Physics, ²Department of Chemistry,

Princeton University, Princeton, New Jersey 08544, U. S. A.

³ Los Alamos National Laboratory, Los Alamos, New Mexico 87544, U.S.A.

⁴Princeton Materials Institute, Princeton University, Princeton, New Jersey 08544, U. S. A.

(Dated: November 4, 2019)

Experiments on the Hall coefficient R_H and heat capacity C reveal an unusual, compensated electronic ground state in the ruthenate $\text{Bi}_3\text{Ru}_3\text{O}_{11}$. At low temperature T , R_H decreases linearly with magnetic field $|H|$ for fields larger than the field scale set by the Zeeman energy. The results suggest that the electron and hole populations are tuned by H in opposite directions via coupling of the spins to the field. As T is decreased below 5 K, the curve $C(T)/T$ vs. T^2 shows an anomalous flattening consistent with a rapidly growing Sommerfeld parameter $\gamma(T)$. We discuss shifts of the electron and hole chemical potentials by H to interpret the observed behavior of R_H .

PACS numbers: 72.15.-v, 72.60.+g, 71.27.+a

INTRODUCTION

The layered ruthenates have gained increased attention because of the discovery of superconductivity with triplet spin pairing in Sr_2RuO_4 [1], metamagnetism [2] as well as field-tuned quantum critical behavior [3] in $\text{Sr}_3\text{Ru}_2\text{O}_7$, and unusual ferromagnetism in SrRuO_3 [4, 5]. Recently, a ruthenate from a different structural family $\text{La}_4\text{Ru}_6\text{O}_{19}$ has gained prominence because it exhibits non-Fermi liquid behavior at low temperatures [6]. This oxide has the KSbO_3 structure which consists of a three dimensional network of edge-sharing and corner-sharing RuO_6 octahedra. In this structure, a network of short Ru-Ru bonds co-exists with a network of Ru-O-Ru bonds. The mix of nearly localized states centered on the short (2.49 Å) Ru-Ru bonds and delocalized states derived from the Ru-O-Ru bonds is rare in transition-metal oxides. The interaction between them is analogous to that between f electrons and s electrons in heavy-fermion materials. Distinct signatures of anomalous behavior are observed in $\text{La}_4\text{Ru}_6\text{O}_{19}$. The heat capacity $C(T)$ displays a $T \log T$ profile below 1 K in zero magnetic field. The resistivity ρ shows a T -linear dependence below 30 K that extrapolates to zero as $T \rightarrow 0$ (with no measurable residual resistivity), which is a clear signature of non-Fermi liquid behavior. By contrast, these anomalous properties are absent in the closely related compound $\text{La}_3\text{Ru}_3\text{O}_{11}$ in which the Ru-Ru distance is much longer (2.99 Å). The anomalous electronic properties of $\text{La}_4\text{Ru}_6\text{O}_{19}$ are crucially dependent on the presence of the narrow peak in the density-of-states derived from the Ru-Ru dimers.

We have synthesized a third member [7] of this family $\text{Bi}_3\text{Ru}_3\text{O}_{11}$ in which the Ru-Ru distance (2.61 Å) lies between those of the previous two. Heat capacity measurements reveal that, at low T , the Sommerfeld parameter γ increases as T decreases below 5 K. The Hall coefficient $R_H(H)$ reveals that the ground state is compensated but the relative electron and hole populations are highly sen-

sitive to the field \mathbf{H} . In relatively weak H , $R_H(H)$ decreases linearly with increasing $|H|$, implying that the electron and holes populations are tuned in opposite directions.

HEAT CAPACITY AND RESISTIVITY

Polycrystalline samples of $\text{Bi}_3\text{Ru}_3\text{O}_{11}$ were prepared by pressing high-purity $\text{Bi}_3\text{Ru}_3\text{O}_{11}$ powder under 50 kbar at 700 C for 2 h, and then annealing overnight at 900 C under ambient pressure. Details of the sample preparation, structural and thermodynamic measurements are reported elsewhere [8]. The low-temperature heat capacity $C(T)$ of $\text{Bi}_3\text{Ru}_3\text{O}_{11}$ is plotted as $C(T)/T$ vs. T^2 in Fig. 1. The curve starts out nominally linear above 5 K with an apparent extrapolated intercept at the value ' γ ' = 5.3 mJ/mol Ru K². However, below 5 K, the curve flattens out to a much less T -dependent line that extrapolates at $T = 0$ to the value $\gamma = 28$ mJ/mol Ru K², which is ~ 3 times smaller than in $\text{La}_4\text{Ru}_6\text{O}_{19}$. The value of γ is enhanced by a factor of 4-5 over that in conventional metals, but less than that in heavy-fermion systems (for which $\gamma \sim 300$ -1500 mJ/mol K²). The highly unusual feature of $C(T)/T$ is the weak T dependence of the curve at low T . The straight line corresponding to the usual phonon contribution varying as T^3 is absent. We interpret the relative flat curve below 5 K as a gradual crossover to an unusual electronic state in which the carrier effective mass m^* rises by a factor of ~ 5 to raise γ to its value at $T = 0$. The unusual nature of the ground state becomes apparent in the Hall results reported in the next section.

As in $\text{La}_4\text{Ru}_6\text{O}_{19}$ and $\text{La}_3\text{Ru}_3\text{O}_{11}$, the resistivity ρ is metallic. In our polycrystalline sample, however, the residual resistivity ratio (RRR ~ 13) is smaller because of significant scattering from disorder and impurities. As T falls from 300 to 120 K, ρ initially decreases linearly with T (Fig. 2). Below 100 K, ρ drops rapidly to the

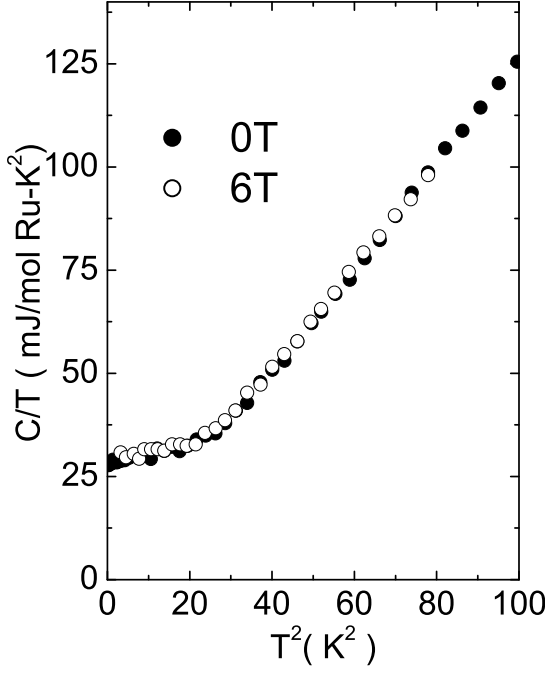


FIG. 1: Plot of the low- T heat capacity $C(T)$ as $C(T)/T$ vs. T^2 in $\text{Bi}_3\text{Ru}_3\text{O}_{11}$ in zero field (solid circles) and in a 6-T field (open). Below 5 K, the curves flatten out to yield a relatively large Sommerfeld constant $\gamma = 28 \text{ mJ/mol Ru-K}^2$.

residual value ρ_0 . The variation below 25 K is nearly linear in T^2 but deviates below 5 K (see inset to Fig. 2). The bulk susceptibility χ measured in a SQUID magnetometer with $H = 1$ T rises gradually to the value $3 \times 10^{-4} \text{ emu/G.mol Ru}$ as T is cooled from 400 K to 25 K, consistent with Pauli susceptibility [8]. Below 25 K, however, we observe a steep increase suggestive of spin fluctuations. However, there is little evidence for local moments or magnetic ordering in χ (at 5 K, χ remains independent of H up to 5 T and corresponds to $0.004 \mu_B$ per Ru ion at 5 T).

HALL EFFECT AND MAGNETORESISTANCE

The Hall effect and magnetoresistance together provide a powerful way to probe the nature of the electronic state at low T . At temperatures 50 to 300 K, we find that the Hall resistivity ρ_{xy} is strictly linear in H (data not shown). Above 200 K, the Hall coefficient $R_H = \rho_{xy}/H$ is positive and approaches the T -independent value $0.72 \times 10^{-9} \text{ m}^3/\text{C}$ (corresponding to a Hall number $n_H = 8.7 \times 10^{21} \text{ cm}^{-3}$). At 110 K, R_H changes sign, implying that electron-like and hole-like Fermi Surfaces (FS) are present. Interestingly, below 50 K, the curve of ρ_{xy} vs. H rapidly acquires pronounced curvature in fields of 1-3 T (Fig. 3). Such highly pro-

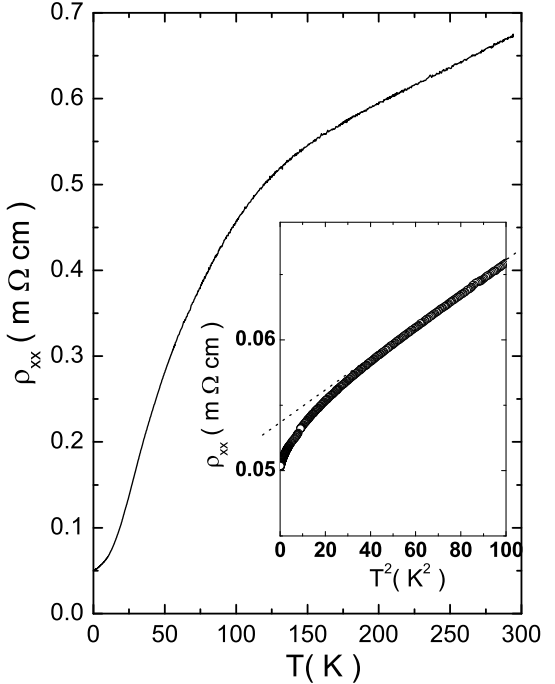


FIG. 2: The T dependence of the resistivity ρ in $\text{Bi}_3\text{Ru}_3\text{O}_{11}$. Between 5 and 25 K, ρ fits well to a T^2 dependence, but shows a slight downwards deviation below 5 K (inset).

nounced curvature, strikingly unusual in a system with such a short mean-free-path ℓ (500-900 Å), signals that the applied field strongly affects the electronic state itself. Below 50 K, the observed Hall signal is the combined effect of H exerting a Lorentz force on the carriers and simultaneously altering the ground state.

To verify this, we divide $\rho_{xy}(H)$ by H to define the *field-dependent* Hall coefficient $R_H(H) = \rho_{xy}/H$ (Fig. 4). This removes the leading H -linear factor in ρ_{xy} leaving an $R_H(H)$ that is even in H (we have folded the curves about the axis $H = 0$ in Fig. 4 to emphasize this point). As indicated by the dashed lines, $R_H(H)$ is linear in $|H|$ at high fields, but as $H \rightarrow 0$, it deviates downwards consistent with a ‘rounding’ in weak fields (we associate this rounding with thermal broadening). As discussed below, these features strongly suggest that the field increases the electron-like population while diminishing the hole-like population via Zeeman coupling to the spins of the carriers.

At each T , the curves in Fig. 4 are characterized by two parameters, the zero-field Hall coefficient $R_H^0(T)$ and the slope of the dashed lines $\mathcal{P}(T) \equiv |dR_H/dH|$ (evaluated at 14 T). At the lowest T , R_H^0 falls steeply with increasing T (solid symbols in Fig. 5). As the carrier lifetimes are not T dependent in the impurity scattering regime, this rapid variation cannot arise from changes to ℓ . Instead, it comes from changes to the density of states

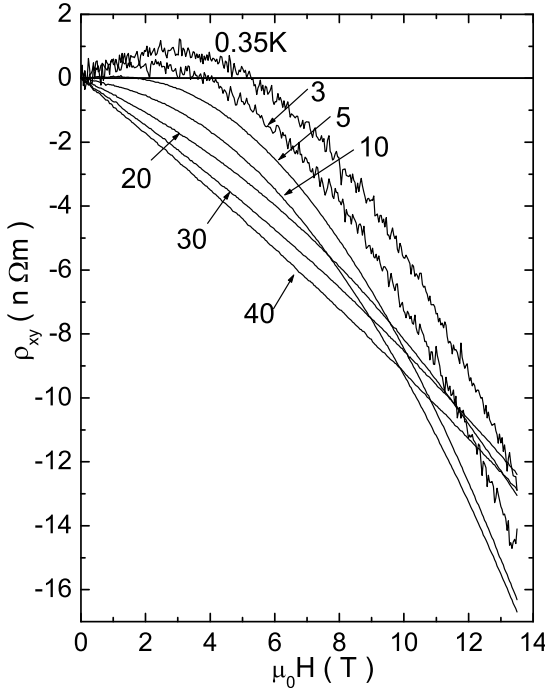


FIG. 3: Curves of ρ_{xy} vs. H in $\text{Bi}_3\text{Ru}_3\text{O}_{11}$ showing unusually pronounced curvature vs. H below 50 K. The weak-field slope $\partial\rho_{xy}/\partial H$ increases steeply with T as $T \rightarrow 0$. Above 50 K, ρ_{xy} is strictly linear in H to 14 T.

(DOS) in the electron and hole bands at finite T . The second parameter $\mathcal{P}(T)$ measures the rate of decrease in R_H with increasing H . As T is decreased from 50 K, $\mathcal{P}(T)$ grows gradually (open symbols in Fig. 5), but saturates to a constant near 5 K. The saturation of $\mathcal{P}(T)$ at low T recalls the behavior of $C(T)/T$ in Fig. 1. Before discussing the Hall results further, we consider the magnetoresistance (MR).

Figure 6 shows the transverse MR $[\Delta\rho/\rho]_{\perp}$ (measured with $\mathbf{H} \perp \mathbf{I}$ with \mathbf{I} the applied current) and the longitudinal MR $[\Delta\rho/\rho]_{\parallel}$ (measured with $\mathbf{H} \parallel \mathbf{I}$) at low T . As $\mathbf{H} \parallel \mathbf{I}$ in the longitudinal MR geometry, the field couples onto to the spin degrees of freedom (either of the carrier or local moments that scatter the carriers). At each T , the orbital component may be isolated by subtracting the longitudinal MR signal from the transverse [9]. In plotting $[\Delta\rho/\rho(0)]_{orb}$ against $H/\rho(0)$ (Kohler plot), we find that curves taken at different T all collapse together. The Kohler scaling confirms that the orbital component of the MR arises entirely from the effect of the Lorentz force on the electron trajectory (classical MR). The magnitude of $[\Delta\rho/\rho(0)]_{orb}$ places an upper bound for the value of ℓ_0 of 900 Å, which is rather short, and consistent with the modest RRR.

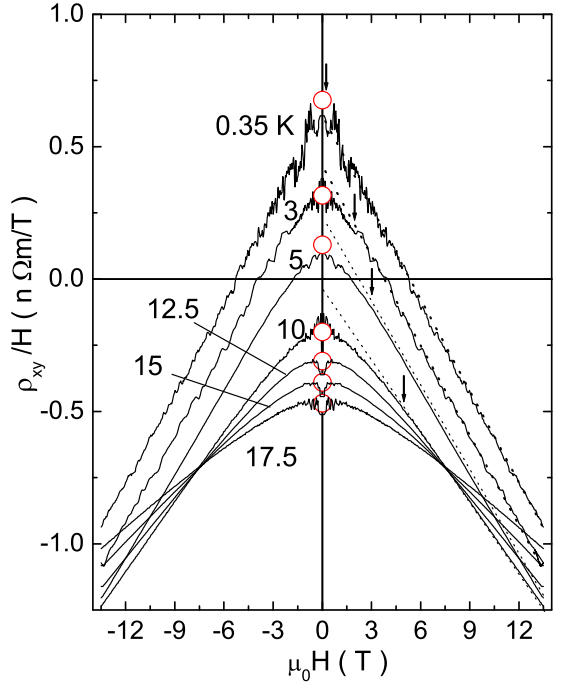


FIG. 4: Replot of ρ_{xy} as $R_H(H) = \rho_{xy}/H$ vs. H . At each T , we have reflected the *same* curve about $H = 0$ to emphasize that R_H is symmetric in H . At large H , R_H is strictly linear in H (dashed lines), but below the Zeeman field scale H_Z (arrows), $R_H(H)$ deviates from the dashed line because of thermal broadening. Open circles represent R_H^0 .

FIELD-EFFECT ON CARRIER POPULATIONS

The Hall results in Fig. 4 imply that an applied field alters the *relative* electron and hole populations linearly at large H . The MR results (Fig. 6), however, show that the change to the combined carrier population is negligible even at our lowest T . Since the decrease in $R_H(H)$ is rigorously linear in H at large enough fields, the changes induced by field must arise from the coupling of H to the carrier spins by their Zeeman energy. For the field to be effective, the Zeeman energy must clearly exceed $k_B T$, i.e. H must exceed the Zeeman field scale $H_Z = k_B T/g\mu_B$ where k_B is Boltzmann's constant, g is the Lande g-factor and μ_B the Bohr magneton. Examination of the curves of R_H in weak fields shows that this is indeed the case. At each T , R_H deviates from the dashed lines when $H < H_Z$ (arrows in Fig. 4). For simplicity, let us assume a two-band model, in which σ^i and σ_H^i are, respectively, the conductivity and Hall conductivity in the electron-like band ($i = e$) or hole-like band ($i = h$). In the impurity scattering regime, the mean-free-path is a \mathbf{k} -independent length ℓ_0 that has the same value in both bands. We may then write for the i^{th}

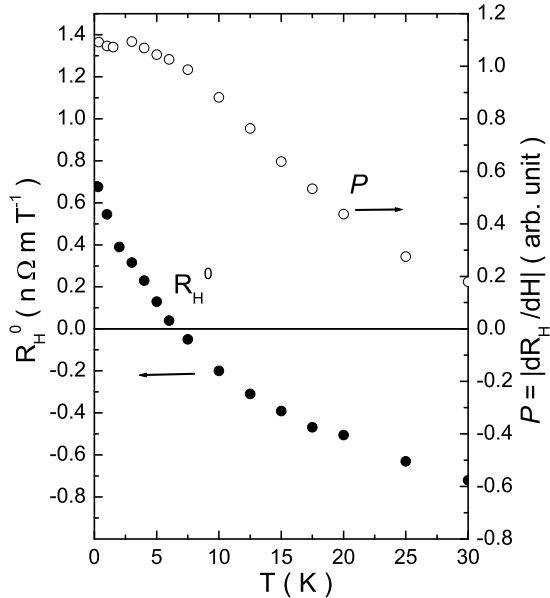


FIG. 5: The T dependence of the zero-field Hall coefficient $R_H^0(T) = \rho_{xy}/H$ ($H \rightarrow 0$) (solid symbols) and $\mathcal{P}(T) \equiv |dR_H/dH|$ evaluated at 14 T (open symbols) below 30 K. At low T (0.35–5 K), the steep decrease of R_H^0 arises from changes to the DOS. The parameter \mathcal{P} is the change in $R_H(H)$ induced by unit H .

band [10]

$$\sigma^i = g\mathcal{S}_i\ell_0, \quad \sigma_H^i = g\mathcal{S}_i \frac{eH}{\hbar k_{F,i}} \ell_0^2 \equiv \pm g\mathcal{R}_i H \ell_0^2, \quad (1)$$

where $g = e^2(12\pi^3\hbar)^{-1}$, \mathcal{S}^i is the ‘transport weighted’ Fermi Surface area of the i^{th} band, $k_{F,i}$ the average Fermi wavevector, and the $+$ ($-$) sign applies to σ_H^h (σ_H^e). For isotropic bands, the quantity \mathcal{R}_i may be regarded as proportional to DOS of the i^{th} band. In this limit, R_H is independent of ℓ_0 , viz.

$$R_H(H) = \frac{(\sigma_H^e + \sigma_H^h)}{[H(\sigma^e + \sigma^h)^2]} \rightarrow \frac{\mathcal{R}_h(H) - \mathcal{R}_e(H)}{g(\mathcal{S}_h + \mathcal{S}_e)^2}, \quad (2)$$

As the orbital MR is weak, we may ignore the effect of H on the denominator in Eq. 2. The linear decrease in R_H at large H then implies that both \mathcal{R}_e and \mathcal{R}_h must vary linearly with H , but with opposite signs. At $T = 0$, we have $\mathcal{R}_i(H) = \mathcal{R}_i(0)[1 - \alpha_i|H|]$, with the parameters $\alpha_e < 0$ and $\alpha_h > 0$. In the Drude approximation, \mathcal{R}_i is proportional to the carrier density in the i band. As soon as H is non-zero, the electron population increases linearly while the hole population decreases.

At finite T , thermal broadening makes this field effect insignificant until H exceeds H_Z , as noted. In high fields, the rate at which H alters the relative populations, measured by \mathcal{P} , is independent of T below 5 K (Fig. 5).

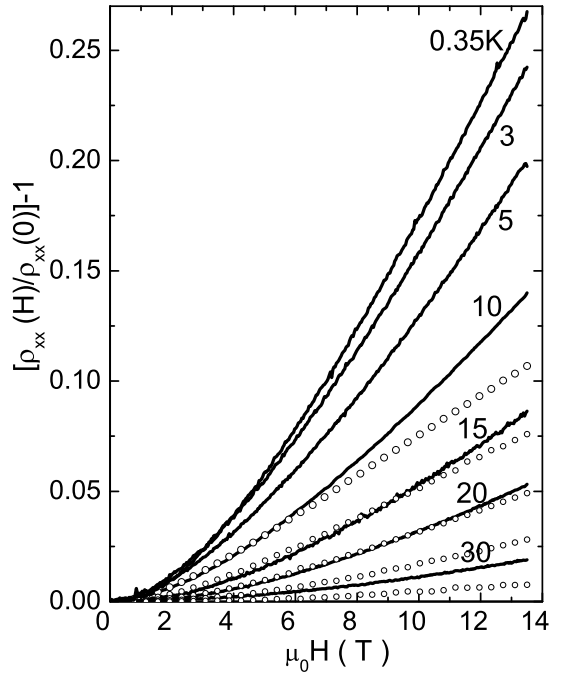


FIG. 6: The transverse magnetoresistance $[\Delta\rho/\rho]_{\perp}$ ($\mathbf{H} \perp \mathbf{I}$) at selected T (solid curves). Curves of the longitudinal MR $[\Delta\rho/\rho]_{\parallel}$ ($\mathbf{H} \parallel \mathbf{I}$) at T at 5, 10, 15, 20 and 30 K, are displayed as small open circles.

Above 5 K, the field sensitivity diminishes gradually, becoming undetectable at 50 K.

DISCUSSION

In analyzing the ρ_{xy} curves, we have ignored the possibility of skew scattering contributions to the Hall current from scattering off local moments or spin fluctuations. In heavy fermion systems, the spin fluctuations of local moments typically dominate the Hall effect, and curvature in ρ_{xy} vs. H may be observed if magnetic ordering is present. For e.g. in CeAl₂, a metamagnetic transition near 5 T strongly affects the curve of ρ_{xy} vs. H [11]. However, as discussed above, the evidence from χ for local moments in Bi₃Ru₃O₁₁ is quite weak. The estimated moment on each Ru ($< 0.004\mu_B$ at 5 K) is far too feeble to produce observable magnetic scattering. More importantly, the behavior of ρ_{xy} with H (and T) in skew scattering has a well-studied characteristic form arising from domain rotation. The linear dependence of ρ_{xy}/H in Fig. 4 is incompatible with this form. The available evidence persuades us that the anomalous behavior in Fig. 4 is unrelated to Hall currents from skew scattering off magnetic moments.

In a paramagnetic one-band metal, the shift in field of the chemical potential μ_+ (μ_-) for spin-up (spin-

down) electrons changes the spin sub-populations by $\delta n_{\pm} = \pm \frac{1}{2} \mathcal{N}_F \mu_B H$, to give the familiar Pauli magnetization $M = \mathcal{N}_F \mu_B^2 H$ (here \mathcal{N}_F is the total DOS at the Fermi level). However, R_H is unaffected because the Hall effect is sensitive to the total population, not δn_{\pm} . For a system with holes and electrons, the argument applies independently to each FS, so R_H remains unchanged. The data in Fig. 4 require an unusual ground state in which the chemical potentials of the holes and electrons (μ_h and μ_e , respectively) behave as if they are Zeeman-coupled to the field with opposite signs, and shift just like μ_{\pm} , viz.

$$\mu_h(H) = \mu_h(0) + \frac{1}{2} g \mu_B H, \quad \mu_e(H) = \mu_e(0) - \frac{1}{2} g \mu_B H. \quad (3)$$

The implication is that, in a field, the hole and electron bands are each spin-polarized, but in opposite directions. In a weak H at $T = 0$, μ_e shifts downwards (this is dictated by the observed decrease in $R_H(H)$) leading to an increase in the electron population, while μ_h shifts upwards leading to a decreased hole population. As ρ is virtually unchanged, the net population change is nearly zero.

The inferred coupling between the hole and electron bands is broadly reminiscent of excitonic condensates [12] involving the pairing of holes and electrons in a compensated semi-metal. Recent work [13] has explored various magnetic ground states. However, our observations do not seem to have been predicted. Moreover, we caution that the opening of an energy gap has not been observed. The nearest feature to an order parameter seems to be \mathcal{P} , which appears near 50 K and gradually increases to saturate at 5 K, a crossover behavior reflected in the heat capacity. Hopefully, the results reported will motivate a search for a correlated state that reproduces the obser-

vations in Fig. 4.

The research reported is supported by a MRSEC grant from the U.S. National Science Foundation (DMR 0213706).

- [1] Y. Maeno *et al.*, *Nature* 372, 532 (1994); For a review, see Y. Maeno in *More is Different*, edited by Ong N. P. and Bhattacharyya R. N. (Princeton Univ. Press Princeton) 2001, p.135.
- [2] Perry R. S. *et al.*, *Phys. Rev. Lett.* 86, 2661 (2001).
- [3] Grifera S. A. *et al.*, *Science* 294, 329 (2001).
- [4] Longo J. M., Raccab P. M. and Goodenough J. B., *Jnl. Appl. Phys.* 39, 1327(1968).
- [5] Allen P. B., Berger H., Chauvet O., Forro L., Jarlborg T., Junod A., Revaz B. and Santi G., *Phys. Rev. B* 53, 4393(1996).
- [6] Khalifah P., Nelson K. D., Jin R., Mao Z. Q., Liu Y., Huang Q., Gao X. P. A., Ramirez A. P. and Cava R. J., *Nature* 411, 669(2001).
- [7] He L., Anderson J. R., Franzen H. F. and Johnson D. C., *Chem. Mater.* 9, 715(1997); Facer G. R., Elcombe M. M. and Kennedy B. J., *Aust. J. Chem.* 43, 1897(1993).
- [8] Haas M. K., Cava R. J., Lee Wei-Li., Ong N. P., Lawes G. and Ramirez A. P. *preprint* (2003).
- [9] Harris J. M. *et al.*, *Phys. Rev. Lett.* 75, 1391(1995).
- [10] Ziman J. M., *Principles of the Theory of Solids*(Cambridge Univ. Press, London) 1972.
- [11] Lapierre F., Haen P., Briggs A. and Sera M., *Jnl. Magn. Magn. Mat.* 63, 76(1987).
- [12] Zhitomirsky M. E., Rice T. M. and Anisimov V. I., *Nature* 402, 251(1999); Zhitomirsky M. E., and Rice T. M., *Phys. Rev. B* 62, 1492(2000).
- [13] Balents Leon and Varma C. M., *Phys. Rev. Lett.* 84, 1264(2000).